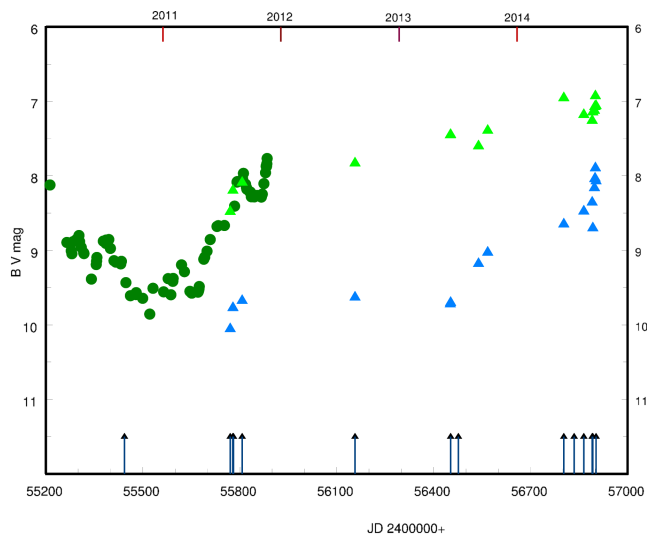


## CH CYGNI: NEW BRIGHTENING IN 2014

RSPAEV, F.; KONDRATYEVA, L.; AIMURATOV, E.

Fessenkov Astrophysical Institute, Almaty, Kazakhstan. e-mail: kondr.lud@gmail.com; lu\_kondr@mail.ru

The brightest symbiotic object CH Cygni has undergone several outbursts. Numerous papers are devoted to the study of this object. A summary of observational history of CH Cyg was presented in the paper of Contini et al. (2009). The last flash took place in 1998-2000 (Skopal et al. 2004) and was followed by a quiescent phase. Then in 2006 a drop to a very low optical state was registered. Later it was interrupted by two short brightenings up to  $\sim 8^m$  in  $V$  filter, observed during 2009 July and from 2009 September to the end of the year (Skopal et al. 2012). Spectral observations are discussed in many papers as well (e.g., Burmeister et al. 2009, and Wallerstein et al. 2010).



**Figure 1.** Light curve of CH Cyg from 2010 to 2014. Photoelectric data and results of CCD photometry from Skopal et al. (2012) are signed by circles and our values by triangles, blue color is used for  $B$  magnitudes and green for  $V$  magnitudes. Dates of our spectroscopic observations are marked by arrows.

Our observations of CH Cyg in Fessenkov Astrophysical Institute were made in 2011-2014. Photometric observations were carried out with two telescopes: 1-meter Carl-Zeiss Jena reflector, equipped with CCD ST-7 (765 $\times$ 510, 9  $\mu$ m) and 70 cm telescope AZT-8, equipped with CCD ST-8 (1530 $\times$ 1020, 9  $\mu$ m) and samples of  $BVR_C$  filters. All

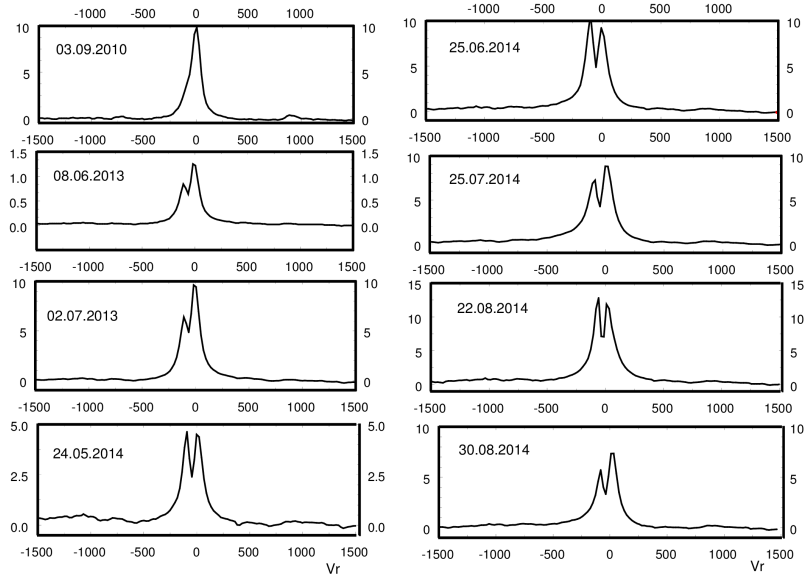


**Figure 2.** Evolution of the H $\alpha$  profiles from a quiescent stage in 2010 to the recent active phase. X-axis shows the heliocentric radial velocity in km/s, Y-axis gives a ratio  $(I_{\lambda} - I_{\text{cont}})/I_{\text{cont}}$ .

Table 1: Photometric results

Date	HJD 2400000+	$B$ mag	$V$ mag	$R$ mag
27.07.2011	55770.479	10.04 $\pm$ 0.05	8.47 $\pm$ 0.03	5.02 $\pm$ 0.01
04.08.2011	55778.521	9.76 $\pm$ 0.05	8.19 $\pm$ 0.02	4.64 $\pm$ 0.01
02.09.2011	55807.125	9.67 $\pm$ 0.04	8.08 $\pm$ 0.03	4.71 $\pm$ 0.01
16.08.2012	56156.190	9.62 $\pm$ 0.04	7.82 $\pm$ 0.01	4.52 $\pm$ 0.01
07.06.2013	56451.400	9.72 $\pm$ 0.04	7.44 $\pm$ 0.02	4.51 $\pm$ 0.01
08.06.2013	56452.260	9.69 $\pm$ 0.04	7.43 $\pm$ 0.01	4.51 $\pm$ 0.01
02.09.2013	56538.370	9.17 $\pm$ 0.03	7.59 $\pm$ 0.02	5.00 $\pm$ 0.02
01.10.2013	56567.085	9.02 $\pm$ 0.02	7.38 $\pm$ 0.02	4.21 $\pm$ 0.01
24.05.2014	56802.383	8.64 $\pm$ 0.02	6.94 $\pm$ 0.02	4.41 $\pm$ 0.01
25.07.2014	56864.250	8.46 $\pm$ 0.01	7.17 $\pm$ 0.01	4.47 $\pm$ 0.01
20.08.2014	56890.208	8.35 $\pm$ 0.01	7.25 $\pm$ 0.02	4.27 $\pm$ 0.01
22.08.2014	56892.153	8.69 $\pm$ 0.02	7.14 $\pm$ 0.02	4.22 $\pm$ 0.01
27.08.2014	56897.149	8.15 $\pm$ 0.03	7.11 $\pm$ 0.02	4.82 $\pm$ 0.01
28.08.2014	56898.177	8.03 $\pm$ 0.01	7.06 $\pm$ 0.02	4.86 $\pm$ 0.01
29.08.2014	56899.142	8.02 $\pm$ 0.01	7.06 $\pm$ 0.01	4.84 $\pm$ 0.01
30.08.2014	56900.148	7.88 $\pm$ 0.02	6.92 $\pm$ 0.01	4.86 $\pm$ 0.01
01.09.2014	56902.129	8.06 $\pm$ 0.03	7.05 $\pm$ 0.02	4.22 $\pm$ 0.01

Table 2: Log of spectral observations

Date	HJD 2400000+	$\Delta\lambda$ Å	Telescope	$R = \lambda/\Delta\lambda$ Å
03.09.2010	55443.140	4400-5200	1-meter	10000
		6100-6900	1-meter	13000
27.07.2011	55770.208	6100-7100	AZT-8	9000
04.08.2011	55778.267	6100-7100	AZT-8	9000
06.08.2011	55780.275	4300-5300	AZT-8	7000
02.09.2011	55807.108	4300-5300	AZT-8	7000
16.08.2012	56156.240	6100-7100	AZT-8	9000
08.06.2013	56452.210	4400-5200	1-meter	10000
		6100-6900	1-meter	13000
02.07.2013	56476.317	6100-6900	1-meter	13000
24.05.2014	56802.346	6100-6900	1-meter	13000
25.06.2014	56834.288	4400-5200	1-meter	10000
		6100-6900	1-meter	13000
25.07.2014	56864.229	4400-5200	1-meter	10000
		6100-6900	1-meter	13000
20.08.2014	56890.200	4300-5300	AZT-8	7000
		6100-7100	AZT-8	9000
22.08.2014	56892.217	4400-5200	1-meter	10000
		6100-6900	1-meter	13000
30.08.2014	56900.150	4400-5200	1-meter	10000
		6100-6900	1-meter	13000

obtained images were dark subtracted and flat fielded. The stars HD195307, HD196330 and HD191418 were adopted as standards. Our observations of CH Cyg were infrequent because the object was in stable stage. The  $BVR_C$  magnitudes are compiled in Table 1. The light curve of CH Cyg for 2010-2014 is presented in Fig. 1. It can be seen that our earlier data, obtained in 2010-2012, agree with values of Skopal et al. (2012) very well.

In the end of May, 2014 the brightening of CH Cyg has started. The maximal values of  $B$  and  $V$  magnitudes ( $B = 7^m88 \pm 0^m02$ ,  $V = 6^m92 \pm 0^m02$ ) are similar to those observed during previous active phases, 1992-1995 and 1998-2000 (Skopal et al. 1997; Skopal 2004). High level of brightness with some fluctuations has been detected to the present.

Spectral observations have been carried out with two spectrographs, attached to the mentioned telescopes and equipped with the CCD cameras ST-8. The slit width equals to 3-4". Wavelength calibration was done using a laboratory source of HeI, NeI and ArI emission lines. Spectra of standard stars obtained just before or after the target were used for the flux calibration. All spectrograms were corrected for atmospheric extinction. The list of observations is presented in Table 2. Spectrograms with a dispersion of 0.5 Å/pixel (1-meter telescope) and 0.75 Å/pixel (AZT-8) were obtained in the “blue” and “red” spectral ranges (Table 2). Emission lines of HI, HeI, [OIII], [NII], FeII, [FeII] were observed in the spectra of CH Cyg. The results of spectral observations are presented in Table 3. Absolute fluxes  $F_{\text{abs}}$  are expressed in  $10^{-10}$  erg cm $^{-2}$ sec $^{-1}$  for H $\alpha$  and  $10^{-11}$  erg cm $^{-2}$ sec $^{-1}$  for other lines. Errors are  $\leq 10\%$  for EWs and about 25% for  $F_{\text{abs}}$  because of non-uniform late-type continuum.

Significant strengthening of all emissions began in 2012. The maximal flux of H $\alpha$  was

Table 3: Spectral results

HJD	H $\beta$		HeI, 4921		[OIII], 5007		H $\alpha$		[NII], 6583		[OI], 6300	
2400000+	$F_{\text{abs}}$	EW	$F_{\text{abs}}$	EW	$F_{\text{abs}}$	EW	$F_{\text{abs}}$	EW	$F_{\text{abs}}$	EW	$F_{\text{abs}}$	EW
	$10^{-11}$	$\text{\AA}$	$10^{-11}$	$\text{\AA}$	$10^{-11}$	$\text{\AA}$	$10^{-10}$	$\text{\AA}$	$10^{-11}$	$\text{\AA}$	$10^{-11}$	$\text{\AA}$
55443.140	1.06	40			0.34	15	0.84	35	0.60	2.8	0.91	7.6
55770.208							0.43	7.5	0.69	1.7		
55778.267							0.41	7.9	0.64	1.3	0.91	4.3
55780.275	0.45	12.3			0.19	7.1						
55807.108	0.39	9.3			0.16	4.1						
56156.240							2.36	47	1.64	3.3	1.30	3.2
56452.210	2.81	16	0.74	2.0	2.00	9.3	3.03	22	0.41	0.3	2.83	6.3
56476.317							3.78	43	0.59	0.7	2.23	8.7
56802.346							17.6	17	1.82	2.4	2.19	4.3
56834.288	5.00	26	1.08	2.4	0.75	4.4	5.34	36	2.70	2.7	2.77	6.8
56864.229	7.30	29	2.28	1.4	2.94	3.5	6.15	49	3.85	3.7	2.09	4.3
56890.200	7.96	18	4.70	4.1	1.26	2.7	6.27	64	5.00	5.1	2.15	4.2
56892.217	9.1	26	3.75	2.9	1.52	2.9	7.19	78	4.35	4.8	2.50	5.8
56900.150	5.08	11	1.73	3.5	0.90	2.8	6.80	63	7.30	7.7	4.94	5.2

Table 4: Radial velocities of the absorption component in the H $\alpha$  profiles

Date	08.06.2013	02.07.2013	24.05.2014	25.06.2014	25.07.2014	22.08.2014	30.08.2014
$V_r$	-63	-63	-46	-53	-49	-34	-36

registered on 24 May 2014. New increase in the emission fluxes of HI, [NII], HeI and [OI] was observed in the end of August. The emission line [OIII], at 5007  $\text{\AA}$  was the strongest earlier – on July, 25, and then its flux decreased (Table 3).

The type of H $\alpha$  profile can be recognized only on spectrograms obtained on the 1-meter telescope with a dispersion of 0.5  $\text{\AA}$ /pixel. Thus, we know that in 2010, H $\alpha$  had a single-peaked profile. Beginning from June, 2013, double-peaked profiles have been observed with variable ratio of “blue” to “red” intensities (Fig. 2). Three possible types of profile are presented in Fig. 2:  $V < R$ ,  $V = R$  and  $V > R$ . Heliocentric radial velocities of absorption lines were measured with an uncertainty of about 0.5  $\text{\AA}$  or  $\pm 20$  km/sec. The obtained values are presented in Table 4.

All observable characteristics of CH Cyg: increasing brightness, strengthening of the emission lines, and double-peaked profiles of Balmer lines testify a new active phase of the object.

#### References:

- Burmeister, M., Leedjarv, L., 2009, *A&A*, **504**, 171  
 Contini, M., Angeloni, R., and Rafanelli, P., 2009, *AN*, **330**, 816  
 Skopal, A., 1997, *IBVS*, **4495**  
 Skopal, A., Pribulla, T., Vanko, M. et al., 2004, *CoSka*, **34**, 45  
 Skopal, A., Shugarov, S. et al. 2012, *AN*, **333**, 242  
 Wallerstein, G., Munari, U., Siviero, A. et al., 2010, *PASP*, **122**, 12